Soils and Foundations 2015;55(5):1148–1157

HOSTED BY

ELSEVIER

CrossMark

The Japanese Geotechnical Society

Soils and Foundations

www.sciencedirect.com

journal homepage: www.elsevier.com/locate/sandf

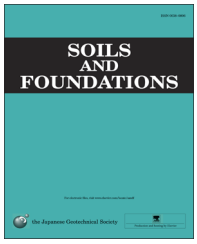

Experimental characterization of the influence of fines on the stiffness of sand with inherent fabric anisotropy

Yan Gao[a], Yu-Hsing Wang[a,*], Jack C.P. Su[b]

[a]*Department of Civil and Environmental Engineering, The Hong Kong University of Science and Technology, Hong Kong Special Administrative Region, China*
[b]*Anderson School of Management, University of New Mexico, Albuquerque, USA*

Received 7 March 2014; received in revised form 6 May 2015; accepted 22 May 2015
Available online 26 September 2015

Abstract

This paper reports the experimental findings regarding the influence of fines on the stiffness reduction, the stiffness anisotropy, and the stiffness changes (during aging) of Toyoura sand and kaolinite (fines) mixtures. The fines content of the mixture samples ranged from 0% to 30% by weight. A tailor-made true triaxial apparatus was used and equipped with a bender element system to measure the shear modulus and with the I-Scan system to monitor the contact forces within the soil sample. By adding fines, the shear moduli of the samples, i.e., G_{hh} and G_{hv} (or G_{vh}), were reduced, such that the higher the fines content, the higher the reduction and the higher the confining pressure, the smaller the reduction. For a given confining pressure σ', the percentage stiffness anisotropy of the samples increased as the fines content was increased from 0% to 2% and then to 8%. As the fines content was increased from 8% to 15%, the percentage stiffness anisotropy gradually decreased. It ultimately reached a small value at which the fines content was 20% where the fines-controlled soil matrix minimized the stiffness anisotropy induced by the inherent fabric anisotropy of sand particles. The aging rates for G_{hh} and G_{hv} were both enhanced after adding fines, and the enhancement was larger as the fines content was increased because the amount of sample creep also increased. A larger amount of sample creep can lead to a greater degree of contact force homogenization which enhances the soil stiffness. This was evidenced by the change in the associated coefficient of variance (CV) of the contact forces measured by the tactile pressure sensors. The aging rate was always greater in G_{hh} than in G_{hv} regardless of the different fines contents. Yet, such aging rate anisotropy became minor as the fines content reached 15%.

Keywords: Fines effects; Fabric anisotropy; Stiffness anisotropy; Aging; Contact forces

1. Introduction

Natural sandy soils often contain different amounts of fines, i.e., silt and clay. Many studies have clearly demonstrated that fines can influence the engineering properties of sandy soils, such as the strength and dilatancy responses, compression behavior, resultant void ratios of compacted samples, and the associated microstructure. Some of these studies and their findings are briefly summarized as follows. Georgiannou et al. (1990) investigated the stress–strain behavior of clayey sand using undrained triaxial tests. For a given granular void ratio, they found that the undrained brittleness and strain to phase transformation increase as the clay content is increased from 4.6% to 10%. When the clay content exceeds 20%, the trend is reversed. When the clay content reaches 30%, the soil sample is no longer dilatant and exhibits a response like that of a sedimented clay. Salgado et al. (2000) performed a series of

*Corresponding author. Fax: +852 2358 1534.
E-mail addresses: cegaoyan@ust.hk (Y. Gao), ceyhwang@ust.hk (Y.-H. Wang), jackcpsu@unm.edu (J.C.P. Su).
Peer review under responsibility of The Japanese Geotechnical Society.

http://dx.doi.org/10.1016/j.sandf.2015.09.015

triaxial and bender element tests to study the effects of fines (silt) on the small-strain stiffness and stress–strain responses of silty sand samples. They demonstrated that the small-strain stiffness decreases dramatically even if there is only a small percentage of silt in the samples. However, the samples become more dilatant and both the peak and the critical-state friction angles increase once the fines content is increased. Vallejo and Mawby (2000) carried out a series of direct shear tests on mixtures of dry Ottawa sand and dry kaolinite and observed that shear strength depends upon the clay (or granular) content. When the fraction of granular material is larger than 75%, the shear strength of the mixture is similar to that of the granular material. When the granular material content is less than 40%, the shear strength of the mixture is then determined by the clay. They also suggested that the minimum porosity of the mixture represents the theoretical boundary between the sand-controlled and the clay-controlled regimes, and that the associated shear strength is maximized when the mixture is prepared at the minimum porosity. Monkul and Ozden (2007) also performed direct shear tests and they too found that the shear strength of a mixture tends to decrease once the fines content of the mixture exceeds the transition value.

Fines may also affect the compression characteristics of coarse-grained soils. Martins et al. (2001) observed that the presence of fines prevents the yielding of a unique compression line for sandy soils. Hence, they suggested that a new framework is needed to model such soils, which do not exhibit the conventional compression behavior. Monkul and Ozden (2007) conducted oedometer tests on reconstituted kaolinite–sand mixtures. Their experimental results demonstrated that the compression behavior of mixtures is mainly dependent on sand before the fines content reaches a transition value. However, once it exceeds this value, kaolinite determines the associated compression behavior instead. The transition value varies between 19% and 34%, depending on the initial conditions, such as the initial void ratio and the stress conditions of the mixture.

The void ratios of compacted coarse-grained soils have also been found to be a function of the fines content (Vallejo and Mawby, 2000; Yang et al., 2006). The resultant void ratios after a sample has been compacted decrease initially with an increasing fines content, but then increase with the further addition of fines. This transition value for the fines content, once again, marks the boundary between the sand-dominated and the fines-dominated soil matrixes. Lade and Yamamuro (1997) suggested that this transition value is larger than 30%. Lade et al. (1998) also offered an explanation for this behavior, namely, that for a soil with a zero fines content, its structure is formed from large (coarse) particles. However, once fines are added to the soil, the pores formed by those large particles will be filled with fines; and therefore, the overall void ratio will decrease. The minimum void ratio is reached when the voids are completely occupied by fines. After this state of minimum void ratio, as the fines continue to jam into the voids, the large particles in the original structure will be pushed apart. Thus, the void ratios are found to increase with the fines content instead. Tanaka et al. (2003) reported that the silt or sand content has an important effect on the pore-size distribution of soils. Zhang and Li (2010) investigated the microstructures of coarse-grained soils with various fines contents. They concluded that a soil sample with a fines content above 30% has a fines-determined microstructure, which exhibits dual-porosity (i.e., containing both intra-aggregate and inter-aggregate pores) and is sensitive to changes in water content. For a soil sample with a fines content below 30%, its soil structure is determined by coarse particles and it is stable despite changes in water content.

Most sand particles are not perfectly round and have different degrees of fabric anisotropy, which in turn can give rise to anisotropic engineering properties, for instance, fabric-induced stiffness anisotropy (e.g., Stokoe et al., 1985; Santamarina et al., 2001; Mitchell and Soga, 2005; Wang and Mok, 2008; Wang and Gao, 2013). However, studies on the effect of fines on the fabric-induced stiffness anisotropy of sandy soils are rare and many questions remain unanswered. For example, does the addition of fines increase or decrease the fabric-induced stiffness anisotropy? What is the transition value of the fines content above which the fabric-induced stiffness anisotropy is minimized? And, how do fines alter the enhancement in stiffness during aging? Here, aging refers to the time-dependent property changes in soils subjected to a constant effective stress (Mitchell and Soga, 2005). Finding the answers to these questions would enable us to gain a more complete understanding of the influence of fines on the engineering properties of sandy soils. Therefore, this serves as the main goal of the present experimental work. Experiments were conducted here using a tailor-made true triaxial apparatus equipped with a bender element system and the I-Scan® system (Tekscan Inc., MA., USA). The bender element system was used to characterize the changes in the small-strain shear moduli in three orthogonal directions after different amounts of fines (kaolinite) were added to Toyoura sand samples that have inherent fabric anisotropy. The time (or aging) effects on the modulus changes were examined in particular, and the corresponding measurements from the I-Scan system served as complementary information to assist with the explanation of the experimental findings. The previous findings in Wang and Gao (2013), regarding the behavior of the stiffness anisotropy of dry, clean Toyoura sand, serve as an important reference and guide to assist in the explanations of the experimental results of this study.

2. Experimental details

2.1. Experimental setup

Fig. 1 presents the experimental setup, which consists of a true triaxial apparatus, a bender element system, and the I-Scan system. Details of the true triaxial apparatus and the bender element system can be found in Wang et al. (2006) or Wang and Mok (2008) and are briefly described in this section to

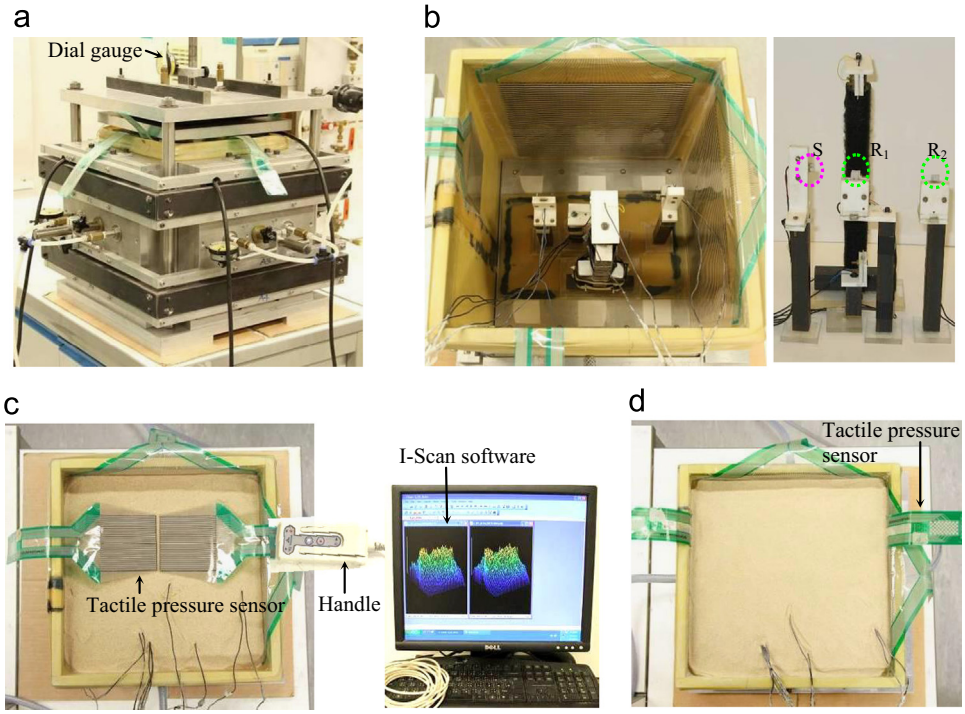

Fig. 1. Experimental setup: (a) true triaxial apparatus (after Wang et al., 2006; Wang and Mok, 2008), (b) the bender element system, (c) the I-Scan system, and (d) tactile pressure sensors buried inside the soil.

facilitate the discussion. The true triaxial apparatus had inner dimensions of 300 × 300 × 300 mm^3. This was also the sample size. The air bag embedded in the device could be pressurized to move the loading plate and then to apply stress onto the soil sample independently in three orthogonal directions. Dial gauges were installed to monitor the sample deformation in the x, y, and z directions. A bender element system was placed inside the true triaxial apparatus to measure the shear wave velocities or the small-strain shear moduli in three directions, i.e., $G_{hh(xy)}$, $G_{hv(yz)}$, and $G_{vh(zx)}$, where the first and second subscripts specify the directions of wave propagation and polarization, respectively, h means the horizontal direction, and v stands for the vertical direction. As illustrated in Fig. 1b, there were three sets of bender elements arranged in three directions. Each set of bender elements consisted of one source, S, and two receivers, R_1 and R_2. Therefore, the corresponding traveling time, t, can be determined by the cross-correlation peak of the two receiver signals to enhance accuracy (Wang et al., 2007). Using Eq. (1), the shear wave velocity and the corresponding small-strain shear modulus can be obtained.

$$G = \rho V_s = \rho\left(\frac{L}{t}\right)^2 \tag{1}$$

where ρ is the soil density and L is the traveling distance. The tip-to-tip distances between the source and the two receiver bender elements were fixed at 75 mm and 150 mm; and therefore, L is the distance between the two receivers, i.e., 75 mm.

The I-Scan® system (Tekscan Inc., MA., USA) was used to capture and record the distribution of contact forces within the soil sample. Note that the system can only measure the contact normal force and not the contact tangential force. As shown in Fig. 1c, in the system, a tactile pressure sensor is connected to the handle, which obtains and processes the measured data and then sends the data to the computer where the results are presented by the provided software. The tactile pressure sensor is ultra-thin and flexible so that it can be buried inside the soil sample (see Fig. 1d) without causing significant disturbance to the stress field. In addition, the tactile pressure sensor was placed above the bender element system; and therefore, the placing of the tactile pressure sensor did not affect the measurements using the bender elements. The tactile pressure sensor used in this study was model 5076 (Tekscan Inc., MA., USA), which has a thickness of 0.1 mm and a sensing area of 83.8 mm × 83.8 mm. This sensor consists of 44 rows and 44 columns of ink traces whose intersecting area functions as a tiny load cell, called a sensel. There are, in total, 1936 sensels in the sensor and each sensel is able to measure the contact force between sand clusters. Sensor calibration was carried out following the procedure suggested by Gao and Wang (2013).

2.2. Testing materials

Toyoura sand was selected as the testing material. Its minimum and maximum void ratios are 0.589 and 0.987, respectively. The mean particle diameter, D_{50}, is equal to 0.21 mm and the coefficient of uniformity, C_u, is 1.53. A Toyoura sand particle has an irregular shape with an aspect ratio roughly ranging from 1.5 to 2.0. The aspect ratio is the

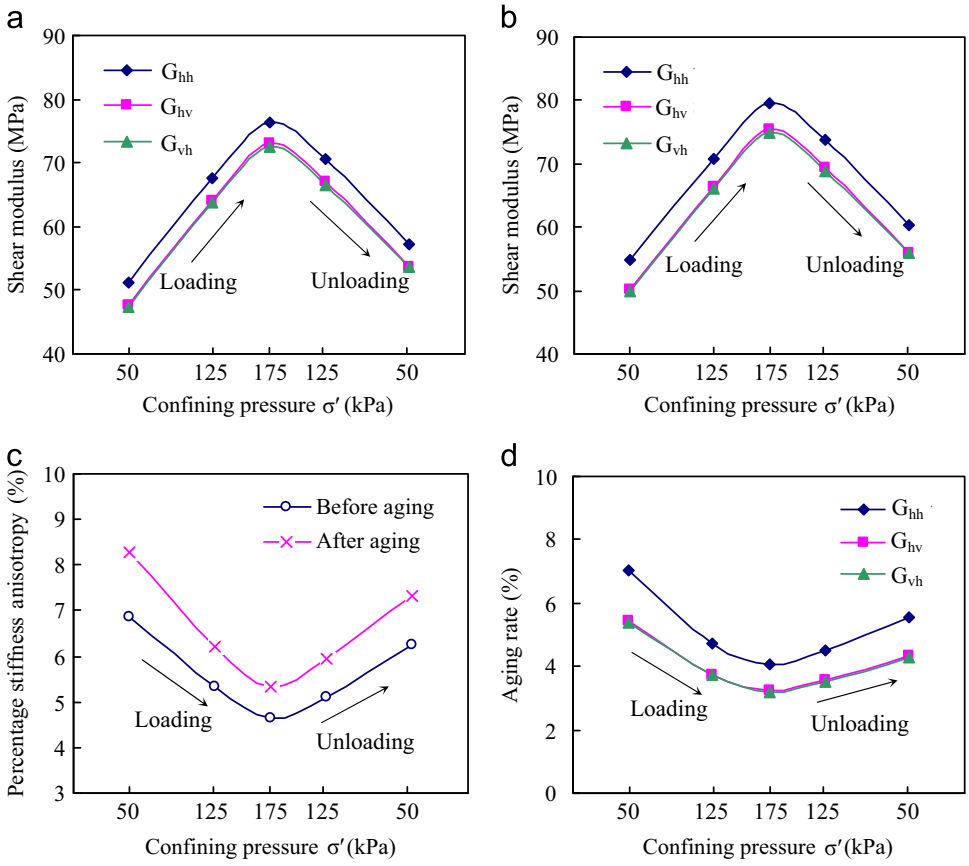

Fig. 2. The stiffness response of the clean Toyoura sand sample: (a) the three shear moduli of the sample without being subjected to aging, (b) the three shear moduli after the sample is subjected to aging, (c) the associated stiffness anisotropy before and after aging, and (d) the associated aging rate. Similar results can also be found in Wang and Gao (2013).

length ratio between the major and the minor axes of the particle. This feature gives rise to the fabric-induced stiffness anisotropy. Dry kaolinite powder (Speswhite Kaolin), of which 90–95% of the particles are smaller than 2 μm, was used as the fines material to be mixed with the Toyoura sand. The kaolinite sample has a liquid limit of 57.9 and a plastic limit of 29.7 (Wang and Siu, 2006). Guided by the previously published results on the transition value of the fines content reviewed in the introduction, samples with different fines contents of 2%, 8%, 15%, 20%, and 30% (by weight) were tested in this study. The response of the dry, clean Toyoura sand sample served as a reference and this sample is denoted as the 0% fines content sample. Note that although only dry samples were tested in this study, the results can still provide preliminary understandings about the influence of fines on the stiffness of sand with inherent fabric anisotropy. Further examinations of samples with different water contents are required since the soil stiffness and the clay behavior are influenced by the water content.

2.3. Sample preparation and experimental arrangement

Soil samples containing Toyoura sand and different amounts of fines were poured into the true triaxial apparatus through a pipe using the air pluviation method. The pipe had an inner diameter of 35 mm and there were layers of sieves put at the bottom of the pipe. In addition, the pluviation height was kept constant ~300 mm. The dry densities of all the testing samples were prepared at a similar value, ~1600 kg/m^3, by controlling the soil weight since the apparatus had a fixed inner size. Considering that Toyoura sand and kaolinite have comparable specific gravity values, i.e., 2.65 and 2.60 for Toyoura sand and the kaolinite, respectively, the void ratios of the samples were therefore also similar, ~0.65. To avoid the bias induced by the anisotropic stress states, isotropic confining pressures σ' were applied, and the loading sequence was 50 kPa→125 kPa→175 kPa→125 kPa→50 kPa. At each loading stage, the three moduli, i.e., $G_{hh(xy)}$, $G_{hv(yz)}$, and $G_{vh(zx)}$, were measured using the bender elements, and the distribution of contact forces within the soil sample was captured by the I-Scan® system. In addition, the confining pressure was kept constant for three days of aging at each loading stage and the shear moduli and the contact force distribution were continuously monitored during the aging period. Note that by considering the time that is required to show a clear aging effect on the stiffness gain and the time that is affordable, the three days of aging were selected for testing. Different experiments have already been carried out to quantify how the effects of aging can influence the increase in stiffness with different aging days for sands, i.e., from 2 to

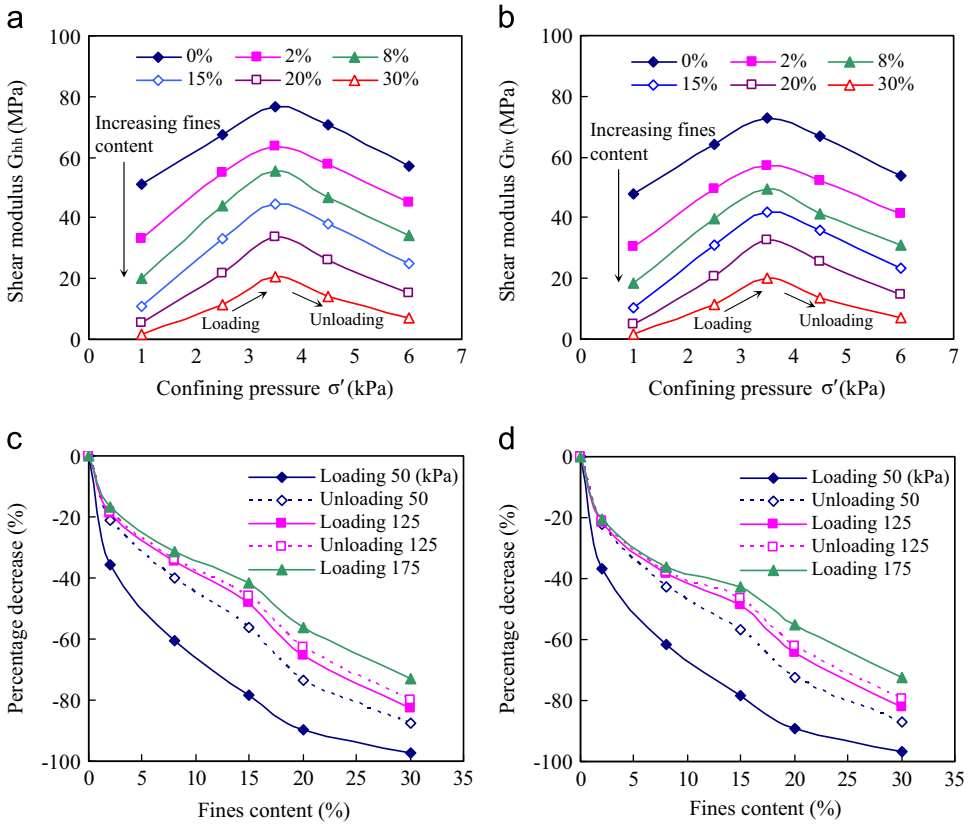

Fig. 3. Influence of fines on the shear moduli of the samples: (a) for G_{hh}, (b) for G_{hv}, (c) the modulus reduction in G_{hh}, and (d) the modulus reduction in G_{hv}.

30 days (see Wang and Tsui, 2009; Gao et al., 2013; Wang and Gao, 2013; Wang et al., 2015). In those experiments, it was observed that the soil stiffness continues to increase with time. Although a sand sample associated with longer aging time can show a more pronounced increase in stiffness, the associated underlying mechanisms are the same as those taking place in the sand sample subjected to a shorter aging period.

3. Experimental results and discussions – the behavior of clean sand

Guided by our previous similar findings in Wang and Gao (2013), and based on the experimental results of this study, the behavior of the stiffness anisotropy of clean Toyoura sand (i.e., the sample with 0% fines content) before and after aging is summarized first to facilitate the following discussion on the influence of fines.

Fig. 2a and c presents the stiffness responses of clean Toyoura sand in response to different levels of confining pressure (without being subjected to the effects of aging). The stiffness anisotropy, i.e., $G_{hh} > G_{hv} \approx G_{vh}$, can be clearly observed (Fig. 2a). Fig. 2c presents the associated stiffness anisotropy in terms of the percentage stiffness anisotropy, which is defined as $(G_{hh}-G_{hv})/G_{hv}$. As confining pressure σ' increases from 50 kPa to 175 kPa during loading, the percentage stiffness anisotropy decreases because the fabric-induced stiffness anisotropy is gradually minimized by the higher confinement. However, as the applied σ' is gradually decreased during unloading, the percentage stiffness anisotropy rebounds.

Once the sample has undergone three days of aging under constant σ', as shown in Fig. 2b and c, not only do the three moduli increase, but the stiffness anisotropy also becomes more pronounced. This behavior can be attributed to the fact that a higher aging rate is associated with G_{hh} than with G_{hv} (or G_{vh}), i.e., G_{hh} increases more than G_{hv} (or G_{vh}) during aging. The aging rate in the figures is presented by $(G_t-G_0)/G_0$ where G_t and G_0 are the modulus at any aging time, t, and the modulus at the initial stage when $t=5$ min, respectively. The DEM simulation results by Gao et al. (2013) and Wang and Gao (2013) demonstrated that as fabric anisotropy (particle aspect ratio) increases, the distribution of contact forces becomes more inhomogeneous and more large tangential forces appear in the horizontal direction (i.e., the x and y directions) than in the vertical direction (i.e., the z direction). This in turn gives rise to a higher sliding creep at particle contacts, and therefore, a larger creep amount in the x and y directions than in the z direction during aging. Note that creep herein follows the general definition whereby soil deformation and movement proceed under a state of constant stress or load (Nowick and Berry, 1972). As a result of a larger creep amount, a higher degree of contact force redistribution, which homogenizes the contact forces and therefore strengthens the soil structure, takes place in the x and y directions than in the z direction. This behavior is reflected in the fact that there is a larger decrease in the coefficient of variance CV (of the contact

forces) in the x and y directions than in the z direction. All of these changes ultimately lead to a higher increase in G_{hh} than in G_{hv} (or G_{vh}) during aging.

The aging rate decreases with increasing confining pressure, as Fig. 2d shows. As also explained in Gao et al. (2013) and Wang and Gao (2013), this is because when a higher confining pressure is applied, on the one hand, the soil sample becomes slightly more densified so that the particle rearrangement is minimized in response to aging; on the other hand, the contact forces become more homogenized, so that less contact force redistribution takes place during aging. This also explains why the sample on the unloading path has a lower aging rate than the sample on the loading path when the two samples are subjected to the same confinement in the experiment.

4. Experimental results and discussions – the influence of fines on stiffness

4.1. Influences of fines on stiffness changes

Fig. 3a and b presents the changes in G_{hh} and G_{hv} after the addition of different fines contents to the samples (before being subjected to the aging effects). The shear moduli are lower for higher fines contents, but still follow the loading and unloading actions to increase and then decrease. The responses of G_{hv} and G_{vh} are always similar, and therefore, only the data for G_{hv} are shown. Fig. 3c and d further summarize the associated percentage decreases in G_{hh} and G_{hv} after adding fines relative to the shear moduli of the sample with zero fines. In general, the amount of modulus reduction decreases with increasing confining pressure. For samples subjected to the same confining pressure, the one on the unloading path experiences a higher modulus reduction because it is densified along the loading path. It is interesting to note that a fines content of only 2% is enough to significantly change the contact stiffness between particles and then the associated small-strain shear modulus, e.g., the decrease in G_{hh} is $\sim$35% under $\sigma' = 50$ kPa (on the loading path).

Since the shear modulus depends on the in-plane stresses, the associated modulus–stress relationship can be described in terms of the mean of the in-plane stress σ'_{mean}, i.e.,

$$G_{hv} = \alpha\left(\frac{\sigma'_v + \sigma'_h}{2\ \text{kPa}}\right)^{\beta} = \alpha\left(\frac{\sigma'_{mean}}{1\ \text{kPa}}\right)^{\beta} \quad (2)$$

and

$$G_{hh} = \alpha\left(\frac{\sigma'_h + \sigma'_h}{2\ \text{kPa}}\right)^{\beta} = \alpha\left(\frac{\sigma'_{mean}}{1\ \text{kPa}}\right)^{\beta} \quad (3)$$

where α and β are constants and are determined from the best fit of the experimental results. The α and β values can capture the contact behavior between particles as well as the packing and the particle properties: the stiffer the particles and the denser the packing, the higher the value of α and the lower the β exponent (Santamarina et al., 2001). Fig. 4 summarizes the variations in α and β values in the modulus–stress relationships for both G_{hh} and G_{hv} in response to the addition of fines. A general trend can be identified for both G_{hh} and G_{hv} modulus–stress relationships, namely, as the fines content is increased, the α value decreases and the β exponent increases. That is, the addition of fines promotes a softer matrix and makes the particle contacts become more deformable. Therefore, a lower shear modulus (i.e., a lower α) and a higher level of sensitivity of the modulus to the change in the stress state (i.e., a higher β) is measured. This is similar to the behavior of sand packing when the associated particle sphericity, roundness, and regularity decrease (experimental results in Cho et al. (2006) show such sand behavior).

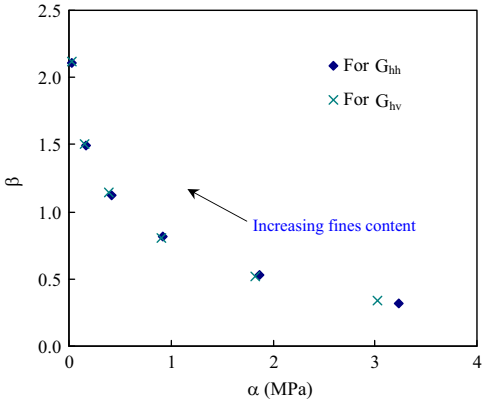

Fig. 4. Variations in the α and β values in the modulus–stress relationships for both G_{hh} and G_{hv} in response to different fines contents. The relationship is obtained based on the measurements on the loading path.

4.2. Influence of fines on stiffness anisotropy under a given confining pressure

Fig. 5 summarizes the associated stiffness anisotropy of the samples with different fines contents. Under a given σ', the stiffness anisotropy initially increases as the fines content is increased from 0% to 2% and then to 8%. Once the fines

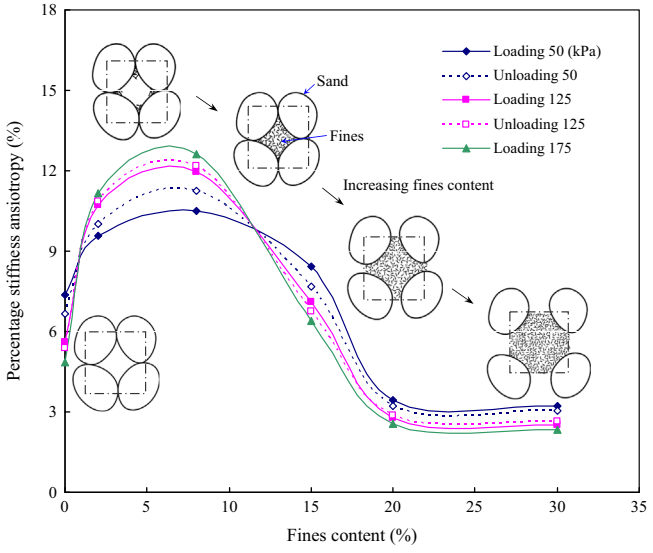

Fig. 5. Summary of the stiffness anisotropy of the samples with different fines contents for a given confining pressure.

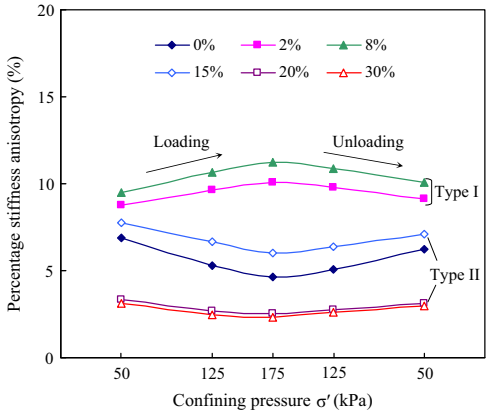

Fig. 6. Summary of the stiffness anisotropy of the samples subjected to different levels of confining pressure for a given fines content.

content is increased beyond 8%, the stiffness anisotropy gradually decreases and ultimately falls to just ~3% as the fines content reaches 20% regardless of the applied confining pressure. As the illustrations in Fig. 5 demonstrate, the fines particles wedge into the regimes around the contact between sand grains. This might strengthen the anisotropic soil structure, and therefore, enhance the stiffness anisotropy. However, as the amount of fines grows, the contact regimes between sand grains will be completely filled and the fines particles will determine the contact behavior and associated shear modulus. That is, the soil structure gradually changes from a sand-controlled matrix to a fines-controlled one. As a result, the stiffness anisotropy due to the inherent fabric anisotropy of sand particles is considerably reduced.

4.3. Influence of fines on stiffness anisotropy under various levels of confining pressures

Fig. 6 presents the percentage stiffness anisotropy for a given fines content in response to different levels of confining pressure during loading and unloading. The soil responses can be categorized into two types depending on the fines content. The type I response is exhibited by the samples with relatively lower fines contents (i.e., the samples with 2% and 8% fines contents). Their stiffness anisotropy behavior is counter to the expectation and different from the responses of clean sand. The percentage stiffness anisotropy increases with increasing σ' instead and vice versa. That is, those fines particles wedged into the regimes around the contact between sand grains could stabilize the anisotropic structure more efficiently as σ' increases. The type II response is observed in the samples with relatively higher fines contents (i.e., the samples with 15%, 20%, and 30% fines contents). The stiffness anisotropy of those samples, similar to that of the clean sand sample, decreases with increasing σ' and vice versa. Once again, when the sample contains a higher fines content, e.g., 20%, the fines control the behavior of the whole soil matrix, and therefore, the

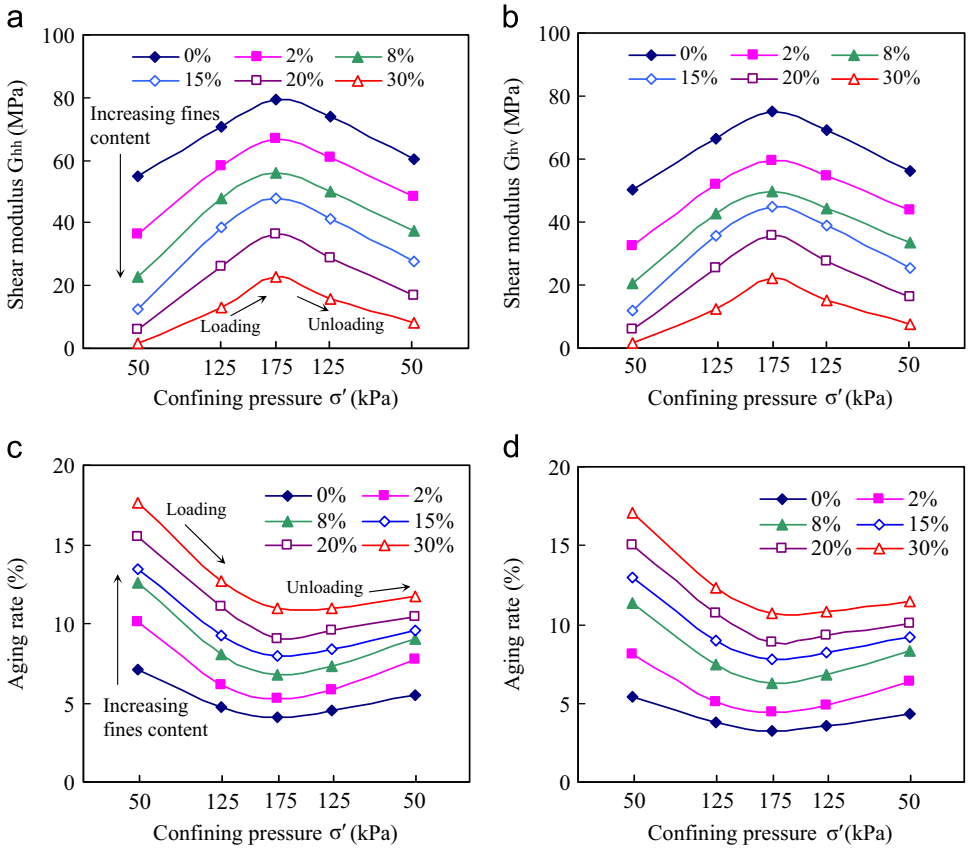

Fig. 7. Influence of fines on the aging behavior: (a) G_{hh} after aging, (b) G_{hv} after aging, (c) aging rate in G_{hh}, and (d) aging rate in G_{hv}.

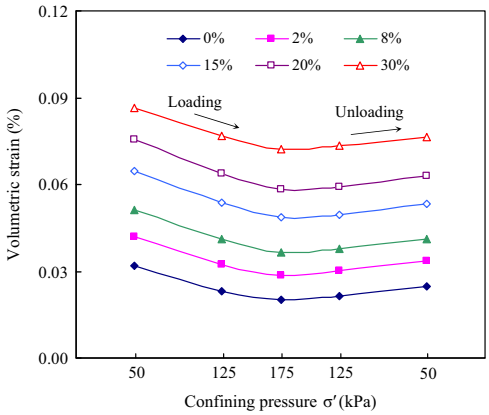

Fig. 8. Volumetric strain induced by three days of aging.

stiffness anisotropy induced by the sand particle becomes minor regardless of the applied confining pressure.

5. Experimental results and discussions – aging behavior

5.1. Effect of fines on the aging rates

Fig. 7a and b summarizes the shear moduli, G_{hh} and G_{hv}, after three days of aging under constant loading, while Fig. 7c and d presents the associated aging rates. The aging rates for both G_{hh} and G_{hv} are enhanced after adding fines and the enhancement is larger as the fines content is increased. This behavior can be attributed to the fact that the amount of sample creep, in terms of volumetric strain, is increased by adding fines materials, as Fig. 8 shows. As a matter of fact, the response pattern of volumetric strain induced by aging perfectly matches that of aging rates. That is, borrowing from the previously discussed concept, a higher amount of sample creep owing to aging leads to a greater degree of contact force homogenization to further stabilize the soil structure; therefore, a greater increase in modulus and the associated aging rate is measured. The phenomenon of contact force homogenization is reflected in the decreasing trend of the associated coefficient of variance (CV) as revealed by Gao et al. (2013) in their DEM simulations. Fig. 9 summarizes the CV values of the contact forces measured by the tactile pressure sensors in samples with different fines contents. Fig. 9a shows the CV values of the measurement before aging, i.e., the initial value, while Fig. 9b shows the associated percentage change in CV after three days of aging. The negative percentage changes in Fig. 9b indicate that the contact forces become more homogenized after aging. As expected, for a given confining pressure, the percentage change in CV induced by the aging effects becomes more negative as the fines content is increased.

As demonstrated in Fig. 7c and d, under a given fines content, similar to the behavior of clean Toyoura sand, the aging rate decreases with increasing confining pressure. In addition, the sample on the unloading path has a lower aging rate than the sample on the loading path. All of these responses can be attributed to the densification effect (Gao et al., 2013). As noted before, after the sample is densified by a higher

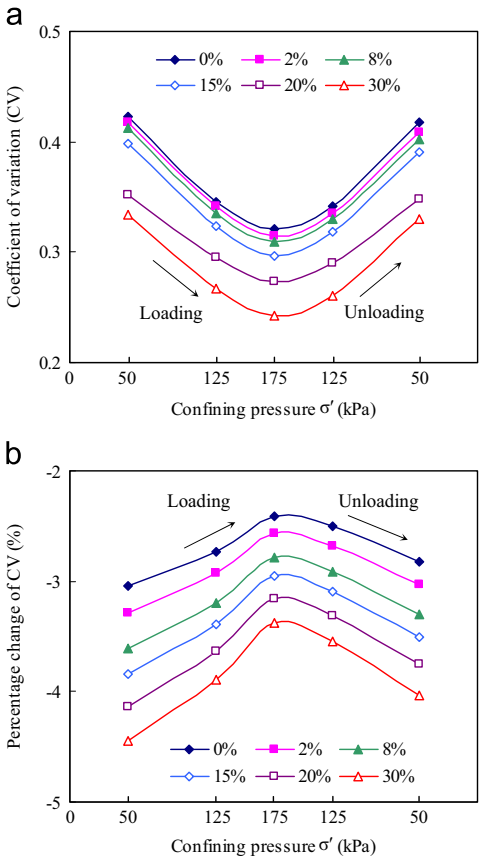

Fig. 9. Contact forces of the samples with different fines contents measured by the tactile pressure sensor: (a) the associated coefficient of variation (CV) before aging and (b) the percentage change of CV after three days of aging.

confining pressure or prior loading, the contact forces become more homogenized so that less contact force redistribution occurs during aging. This in turn gives rise to a smaller change in the associated CV values as evidenced by the results in Fig. 9b. Indeed, a good agreement exists between the aging rate responses in Fig. 7d and the percentage changes in CV due to aging in Fig. 9b. That is, as also noted previously, a greater degree of contact force homogenization gives rise to a larger decrease in CV and a higher aging rate.

5.2. Influence of fines on aging rate anisotropy under a given confining pressure

For the samples with different fines contents under a given confining pressure, the aging rate is always greater in G_{hh} than in G_{hv}, just like that of clean sand. Fig. 10 presents this result in terms of the parameter, the percentage anisotropy of the aging rate. This parameter is defined as the aging rate in G_{hh} minus the aging rate in G_{hv}, normalized by the aging rate in G_{hh}. As observed in Fig. 10, the percentage anisotropy of the aging rate decreases as the fines content increases and becomes very small, ~3%, once the fines content reaches 15% at which point fines dominate the creep behavior of the sample. Note that all the data in Fig. 10 show the non-zero percentage anisotropy of the aging rate, and therefore, imply that the

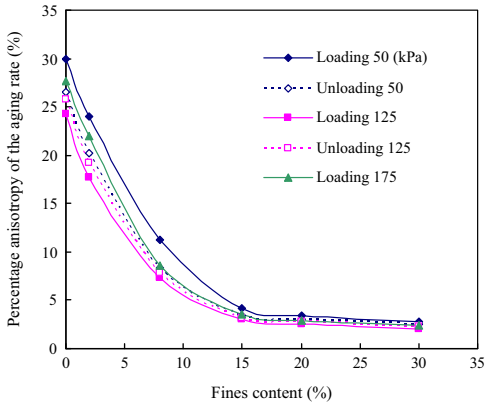

Fig. 10. Summary of the aging rate anisotropy of the samples with different fines contents for a given confining pressure.

stiffness anisotropy is always enhanced after aging regardless of the fines content.

5.3. Influence of fines on aging rate anisotropy under various levels of confining pressures

Fig. 11 presents the percentage anisotropy of the aging rate for a given fines content in response to different levels of confining pressure during loading and unloading. Different from the behavior shown in Fig. 6, regarding the influence of fines on the stiffness anisotropy, all of the samples demonstrate the same trend irrespective of the fines content. The percentage anisotropy of the aging rate decreases with increasing confining pressure and vice versa. Once again, the aging rate anisotropy becomes minor as the fines content reaches 15% when fines dominate the creep behavior of the sample.

6. Conclusions

In this study, the influence of fines on the stiffness reduction, stiffness anisotropy, and stiffness changes (due to aging effects) of Toyoura sand and kaolinite mixtures was examined experimentally. The salient findings are summarized as follows.

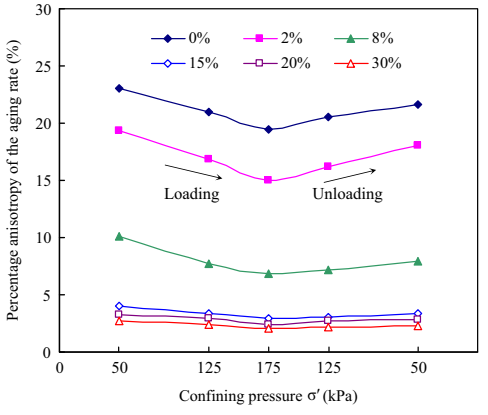

Fig. 11. Summary of the aging rate anisotropy of the samples subjected to different levels of confining pressure for a given fines content.

The shear moduli of the soil samples, i.e., G_{hh} and G_{hv} (or G_{vh}), can be decreased by the addition of fines. The amount of modulus reduction increases with the increasing fines content and decreases with increasing confining pressure. Based on the changes in α and β values of the modulus–stress relationship, the addition of fines indeed promotes a softer matrix and makes the particle contacts more deformable. As a result, a lower shear modulus (i.e., a lower α) and higher sensitivity of the modulus to the stress state (i.e., a higher β) is measured. For a given confining pressure σ', the percentage stiffness anisotropy of the samples initially increases as the fines content increases from 0% to 2% and then to 8%. That is, the fines particles wedged into the regimes around the contact between sand grains could help stabilize the anisotropic structure and enhance the stiffness anisotropy. However, as the fines content of the sample is further increased from 8% to 15%, the associated percentage stiffness anisotropy gradually decreases and ultimately falls to a small value as the fines content reaches 20%. That is, the soil structure is finally changed from a sand-controlled sand matrix to a fines-controlled one. As a result, the stiffness anisotropy due to the inherent fabric anisotropy of the sand particles is considerably reduced.

The increase in shear moduli induced by the aging effects, i.e., the aging rate, is enhanced for both G_{hh} and G_{hv} after the adding of fines, and the enhancement is larger as the fines content is increased. This behavior can be attributed to the fact that the amount of sample creep taking place during the aging period is increased as the fines content is increased. A larger amount of sample creep can lead to a greater degree of contact force homogenization, which is evidenced by the change in the associated coefficient of variance (CV) of the contact forces measured by the tactile pressure sensors. As a result of contact force homogenization, the soil structure is enhanced and so is the associated stiffness. Indeed, the aging rate responses and the percentage changes in CV exhibit the same trend. Regardless of the fines contents and applied confining pressure, the aging rate is always greater in G_{hh} than in G_{hv} just like that of clean sand, i.e., G_{hh} increases more than G_{hv} during aging. That is, the effects of aging can enhance the stiffness anisotropy. However, it should be noted that the difference between the aging rates associated with G_{hh} and G_{hv} narrows to about 3% as the fines content reaches 15%.

Acknowledgments

This research was supported by the Hong Kong Research Grants Council (HKUST9/CRF/09 and HKUST6/CRF/12R) and the HKUST Post-Doctoral Fellowship Matching Fund. The writers are grateful to the reviewers for their valuable comments.

References

Cho, G.C., Dodds, J., Santamarina, J.C., 2006. Particle shape effects on packing density, stiffness, and strength: natural and crushed sands. J. Geotech. Geoenviron. Eng. 132 (5), 591–602 ASCE.

Gao, Y., Wang, Y.H., 2013. Calibration of tactile pressure sensors for measuring stresses in soils. Geotech. Test. Journal 36 (4), 568–574.

Gao, Y., Wang, Y.H., Su, J.C.P., 2013. Mechanisms of aging-induced modulus changes in sand under isotropic and anisotropic loading. J. Geotech. Geoenviron. Eng., ASCE 139 (3), 470–482.

Georgiannou, V.N., Burland, J.B., Hight, D.W., 1990. The undrained behavior of clayey sands in triaxial compression and extension. Géotechnique 40 (3), 431–449.

Lade, P.V., Yamamuro, J.A., 1997. Effects of non-plastic fines on static liquefaction of sands. Can. Geotech. J. 34 (6), 918–928.

Lade, P.V., Liggio Jr, C.D., Yamamuro, J.A., 1998. Effects of non-plastic fines on minimum and maximum void ratios of sands. Geotech. Test. J. 21 (4), 336–347.

Martins, F.B., Bressani, L.A., Coop, M.R., Bica, A.V.D., 2001. Some aspects of the compressibility behaviour of a clayey sand. Can. Geotech. J. 38 (6), 1177–1186.

Mitchell, J.K., Soga, K., 2005. Fundamentals of Soil Behavior, 3rd edition John Wiley & Sons, Inc., New York.

Monkul, M.M., Ozden, G., 2007. Compressional behavior of clayey sand and transition fines content. Eng. Geol. 89 (3–4), 195–205.

Nowick, A.S., Berry, B.S., 1972. Anelastic Relaxation in Crystalline Solids. Academic Press, New York.

Salgado, R., Bandini, P., Karim, A., 2000. Shear strength and stiffness of silty sand. J. Geotech. Geoenviron. Eng., ASCE, 126; 451–462.

Santamarina, J.C., Klein, A., Fam, M.A., 2001. Soils and Waves. John Wiley & Sons, New York.

Stokoe, K.H., Lee, S.H.H., Knox, D.P., 1985. Shear moduli measurements under true triaxial stresses. Advances in the Art of Testing Soils Under Cyclic Conditions: Proceedings of a session/sponsored by the Geotechnical 182 Engineering Division in Conjunction with the ASCE Convention in Detroit, Michigan. ASCE. pp. 166–185.

Tanaka, H., Shiwakoti, D.R., Omukai, N., Rito, F., Locat, J., Tanaka, M., 2003. Pore size distribution of clayey soils measured by mercury intrusion porosimetry and its relation to hydraulic conductivity. Soils Found. 43 (6), 63–73.

Vallejo, L.E., Mawby, R., 2000. Porosity influence on the shear strength of granular material–clay mixtures. Eng. Geol. 58 (2), 125–136.

Wang, Y.H., Gao, Y., 2013. Mechanisms of aging-induced modulus changes in sand with inherent fabric anisotropy. J. Geotech. Geoenviron. Eng., ASCE 139 (9), 1590–1603.

Wang, Y.H., Mok, C.M.B., 2008. Mechanisms of small-strain shear-modulus anisotropy in sands. J. Geotech. Geoenviron. Eng., ASCE 134 (10), 1516–1530.

Wang, Y.H., Lo, K.F., Yan, W.M., Dong, X., 2007. Measurement biases in the bender element test. J. Geotech. Geoenviron. Eng., ASCE 133 (5), 564–574.

Wang, Y.H., Yan, Y.M., Lo, K.F., 2006. Damping-ratio measurements by the spectral-ratio method. Can. Geotech. J. 43 (11), 1180–1194.

Wang, Y.H., Siu, W.K., 2006. Structure characteristics and mechanical properties of kaolinite soils. I. Surface charges and structural characterizations. Can. Geotech. J. 43 (6), 587–600.

Wang, Y.H., Tsui, K.Y., 2009. Experimental characterization of dynamic property changes in aged sands. J. Geotech. Geoenviron. Eng. 135 (2), 259–270.

Wang Y.H., Gao Y. and Ooi G.L., 2015, Experimental characterizations of aging mechanism of sands, J. Geotech. Geoenviron. and Geoenvironmental Engineering, ASCE, http://dx.doi.org/10.1061/(ASCE)GT.1943-5606.0001413,06015016.

Yang, S.L., Lacasse, S., Sandven, R.F., 2006. Determination of the transitional fines content of mixtures of sand and non-plastic fines. Geotech. Test. J. 29 (2), 102–107.

Zhang, L.M., Li, X., 2010. Microporosity structure of coarse granular soils. J. Geotech. Geoenviron. Eng., ASCE 136 (10), 1425–1436.